FR8001915

STATISTICAL MODEL ANALYSIS FOR THE DEEXCITATION OF THE ^{79}Rb FORMED BY THE $^{16}O + ^{63}Cu$ AND $^{32}S + ^{48}Sc$ COMPOUND NUCLEUS REACTION.

J. BARRETO* AND M. LANGEVIN

Institut de Physique Nucléaire,
BP N° 1 91406 Orsay, France

IPNO-PhN-80-14

STATISTICAL MODEL ANALYSIS FOR THE DEEXCITATION OF THE ^{79}Rb FORMED BY THE $^{16}O + ^{63}Cu$ AND $^{34}S + ^{45}Sc$ COMPOUND NUCLEUS REACTION.

J. BARRETO* AND M. LANGEVIN

Institut de Physique Nucléaire - BP.01 - 91406 Orsay, France.

A complete statistical model analysis is presented for the ^{79}Rb compound nucleus formed by the $^{16}O + ^{63}Cu$ and $^{34}S + ^{45}Sc$ reactions on a broad excitation energy interval. Most of all deexcitation channels are compared with the predictions of the codes ALICE and JULIAN. The results show that γ-ray competion with particles emission in the deexcitation of the ^{79}Rb compound nucleus is very important. From these comparisons, a detailed analysis is performed on the approximations made in both evaporation codes.

[Nuclear reactions $^{63}Cu(^{16}O,X)$, $^{34}S(^{45}Sc,X)$ at E^*_{CN} (^{79}Rb) = 40-80 MeV ; complete statistical model analysis of $\sigma(^{16}O,X)$ and $\sigma(^{34}S,X)$.]

INTRODUCTION

The statistical evaporation theory[1] of the compound nucleus has been extended to heavy ions reactions by on one hand the introduction of the angular momentum dependence of the deexcitation mode of the compound nucleus[2,3] and, on the other hand, by the fission channel competition with particles emission in the decay mode of the coumpound nucleus[4,6].

To allow comparison between experiment and theory, several evaporation statistical codes[5-8] have been developed in the past few years, and each of them has different options and assumptions in the manner that calculations are performed. At sufficiently high excitation energy and at large angular momentum, the deexcitation follows different evaporation cascades, involving a large number of nuclei, until a final nucleus is reached. In a complete calculation,

* Fellow of the Conselho Nacional of Desenvolvimento Cientifico E Technologico, Brazil ; and Assistant Associé at Caen University.

the decay of each of these intermediate nuclei has to be taken into account. As this process is very complex, the statistical codes have been built with varied approximations with respect to the statistical theory of the compound nucleus deexcitation.

Many experimental results[8-13] on the cross sections of the deexcitation channels have been compared to different evaporation codes[5-8], but no detailed calculations including all available experimental results have been reported yet, although a systematic study has been made by Gavron[12] with the code JULIAN. Calculations were thus performed with the evaporation codes ALICE[5] and JULIAN[7] and the respective predictions have been compared with experimental results for almost all deexcitation channels of the ^{79}Rb compound nucleus formed by the $^{16}O + ^{63}Cu$ and $^{34}S + ^{45}Sc$ reactions. From these comparisons, attempts are made to shed some light on the assumptions of these statistical codes.

Absolute cross sections have been determined in experiments which were described previously[9,14]. In this study, we concentrate on the comparison between the experimental cross sections of the $^{16}O + ^{63}Cu$ system and the predictions of the code JULIAN (the comparison with the predictions of the code ALICE has already been reported[9]) while for the $^{34}S + ^{45}Sc$ entrance channel, comparison is made with predictions of both the ALICE and JULIAN codes. The choice of these evaporation codes was due, firstly because they are now correctly running at Orsay and also, because they represent two rather different calculations, the former being a very approximate analytical code while the latter is a more rigourous Monte-Carlo one.

CALCULATIONS AND RESULTS

I - THE ALICE CODE

I-1. Method of calculation

The analytical statistical code ALICE running in Orsay is the OVERLAID ALICE version of Blann[15]. Amongst the entrance parameters the choice of the radius r_o and the level density parameter "a" is very important. Indeed, the total reaction cross section is calculated in the parabolic model approximation[16] and the r_o parameter fixes the position of the interaction barrier.

So, in order to obtain agreement with the experimental reaction threshold in the entrance channel, r_o was adjusted at 1,17 fermi for the $^{16}O + ^{63}Cu$ system[9]. However, if we take this same r_o-value for the $^{34}S + ^{45}Sc$, neither is the entrance channel experimental threshold correctly reproduced, nor the energy thresholds of the exit channels. To obtain agreement with the experimental thresholds, r_o was adjusted at 1,26 fermi for the ^{34}S compound nucleus induced reaction.

The level density parameter "a" was taken constant for a fix mass A, whatever the particle emitted. Two trials of calculations were performed : with $a = A/8$ and $a = A/6$, the former value corresponding to a medium level density parameter value[17], while the latter corresponds to the expected value[17] for $A \sim 80$.

The binding energies of the emitted particles were calculated from the subroutine Lymass[15] and it includes shell and pairing corrections. It was also considered that when n, p, d and α-particles were emitted by the compound nucleus, they would take away $2\hbar$, $3\hbar$, $5\hbar$ and $10\hbar$ respectively. Fission competition was included in the calculations for every partial wave.

With respect to the formal statistical compound nucleus deexcitation theory[1-3], the main approximations of the evaporation code ALICE are the following ones :

1) To obtain level densities in the statistical model, it is necessary to calculate effective excitation energies E^*. In the case of particle emission, this excitation energy is that of the residual nucleus after particle evaporation[1]. Once this effective excitation energy is determined, the level densities can be obtained, for example, following Lang's[17] prescription :

$$\rho(E^*,J) = w(E^*,M=J) - w(E^*,M=J+1) \quad , \tag{1}$$

where

$$w(E^*,M) = k \exp\{2[a(E^* - \delta - M^2\hbar^2/2\sigma^2)]^{1/2}\} \times a^{-3/2}\, t^{-3}\, \sigma^{-1/2} \tag{2}$$

is the density of states at the effective energy E^*, and is applied whenever high spins are involved. For small spins and high excitation energies the conventional form[18,19] is used. In the above expression, k is a constant,

δ the pairing energy, $\mathcal{J}$ is the moment of inertia, a is the level density parameter, and τ is the nuclear temperature, related to the excitation energy by :

$$E^* = a\,\tau^2 - 3/2\,\tau + \frac{M^2\hbar^2}{2\mathcal{J}_0} \quad . \tag{3}$$

In ALICE calculations[15], the level densities is determined by the approximate relation :

$$\rho(E^*) = (E^* - E_{ROT})^{-2} \exp\{2[a(E^* - E_{ROT})^{1/2}]\} , \tag{4}$$

which supposes that the rotational energy E_{ROT}, calculated for each partial wave assuming the rigid rotor model, is irrevocably committed to rotational motion and therefore unavailable for particle emission. Thus, the code ALICE works only on excitation energies and the fact of neglecting the angular momentum in the calculations of the level densities can, in consequence, predict unreliable wrong particles emission probabilities, as these probabilities are closely related to the level density $\rho(E,J)$ in the statistical model[1-3] (See below).

2) The emission probability of a particle ν from a compound nucleus to a residual one as energy E_R^* and spin J_R is given, in the statistical model[1-3,6], by :

$$R_\nu(E^*,J;E_R^*,J_R) = \frac{1}{\pi}\,\frac{\rho(E_R^*,J_R)}{\rho(E^*,J)}\,\sum_{S\ell} T_\ell(\varepsilon_\nu) \quad , \tag{5}$$

where S is the channel spin in the exit channel ($\vec{S} = \vec{J}_R + \vec{S}_\nu$) and ℓ, the angular momentum of emitted particle ($\vec{J} = \vec{\ell} + \vec{S}$). $T_\ell(\varepsilon_\nu)$ are the transmission coefficients in the exit channel and $\rho(E_R^*,J_R)$ and $\rho(E^*,J)$ the level densities of the residual nucleus and the compound nucleus, respectively.

In the code ALICE, the relation (5) is remplaced by the nearly identical one :

$$w(\varepsilon)d\varepsilon = (2S+1)\,\mu\,\varepsilon\,\sigma_{inv}(\varepsilon)\,\frac{\rho(E_R^*,J_R)}{\rho(E^*,J)}\,d\varepsilon \tag{6}$$

where $\sigma_{inv}(\varepsilon)$ is the inverse cross section and μ is the reduced mass of the

emitted particle and residual nucleus system. $\sigma_{inv}(\varepsilon)$ is calculated for an energy range $1 \leq \varepsilon \leq 48$ MeV, regardeless the emitted particle, and integrated for all partial waves in the range $1\hbar \leq \ell \leq 17\hbar$ for protons and neutrons, and $1\hbar \leq \ell \leq 30\hbar$ for α-particles. Thus, the emission probabilities calculated by the code ALICE, besides the rough approximation in the determination of the level densities discussed above, are certainly tainted with some discrepancies due to the angular momentum independence in the determination of $\sigma_{inv}(\varepsilon)$ on the emission probabilities calculations.

3) Besides the particles evaporation from a compound nucleus, the statistical theory[1] provides γ-ray decay channel through the emission probability

$$R_\gamma(E^*,J;E_R^*,J_R) = \frac{1}{\hbar} \frac{\rho(E_R^*,J_R)}{\rho(E^*,J)} \sum_L \xi_L \varepsilon_\gamma^{2L+1} \quad , \qquad (6)$$

where L is the multipolarity of the transition and ξ_L is an appropriate normalization constant, which should be derived from experiments. However, in ALICE calculations the γ-decay channel is completely neglected, which is in desagreement with respect to some calculations[6,20,21], where γ-decay were included. These calculations show that γ-ray emissions are very important decay-channels for compound nucleus formed in the vicinity of the Yrast line.

So, the emission probabilities as calculated by the code ALICE are certainly subjected to large uncertainties with respect to the correct statistical model emission probabilities[1-3], due respectively to the rough approximations made in the level densities $\rho(E^*,J)$, in the inverse cross sections $\sigma_{inv}(\varepsilon)$ and, to the neglect of the γ-decay channel.

I-2. Comparison with experimental results

A : $^{16}O + ^{63}Cu$:

With the purpose of clarifying the comparison between statistical code predictions and experiments, a short résumé is given bellow for the $^{16}O + ^{63}Cu$ results[9] and predictions of the code ALICE :

1) For almost all measured evaporation channels the code ALICE correctly predicts the shapes and magnitude of the maximum cross section for these channels

when calculations are performed taking the whole angular momentum distribution of the entrance channels into account. That is setting the cross section for compound nucleus formation egual to the total reaction cross section : $\sigma_{CN} = \sigma_R$.

2) However, while predicting correct cross section for many-particles evaporation channels (Fig.1), the agreement with experimental results worsens with increasing incident energy for few-nucleon deexcitation channels (Fig. 1).

3) In order to obtain agreement between predictions and experiments for these channels, a critical angular momentum energy dependent parameter[9] ℓ_{cr} was introduced in the calculations and the results show that these few-nucleons evaporation channels are very sensitive to this critical angular momentum value used in the calculations (Fig 1), while many-particle channels are insensitive to it.

However, in the light of the above-discussed emission probabilities calculated by the code ALICE, this ℓ_{cr} assumption validity is highly questionable. This question will be discussed latter, in connection with the experimental $^{34}S + ^{45}Sc$ data analysis.

B : $^{34}S + ^{45}Sc$:

The complete calculations for the ^{34}S-induced reaction was performed with the same set of parameter values than for the $^{16}O + ^{63}Cu$ system[9], expect for the interaction barrier r_o-parameter (see above). The detailed comparison (Figs. 2-5) between experimental excitation functions for the $^{34}S + ^{45}Sc$ system and the predictions of the code ALICE give the following results :

1) Calculations performed with the level density parameter $a = A/8$ give predictions in better overall agreement with experimental results than the $a = A/6$ ones. This is illustrated in Figs. 2 and 5, where predictions from the two calculations are compared to two rather different evaporation channels. The agreement between calculated and experimental thresholds, as for the maxima of these excitations fonctions, is worse for $a = A/6$. This is almost a general feature for the other experimental excitation functions. The same behaviour is found for the $^{16}O + ^{63}Cu$ reactions[9], the $a = A/8$ calculations giving close agreement with the experimental results.

2) When calculations are performed setting $\sigma_{CN} = \sigma_R$ (see above) the rising excitation functions parts are correctly reproduced for all deexcitation channels. However, the agreement with experimental results worsens with increasing excitation energy of the compound nucleus, principally for the 2 and 3 nucleons (Fig. 2) and 2 and 3 α-emission channels (Fig. 5). In the first case, the code ALICE overestimates the nucleon emission probability considerably, as it does also in the $^{16}O + ^{63}Cu$ case for the same evaporation channels[9] .

From this results, one would conclude that some critical angular momentum ℓ_{cr} parameter must be introduced in the calculations, in order to limit the formation of the C.N. to ℓ-waves smaller than ℓ_{cr} . Indeed, complete calculations performed with the same set of ℓ_{cr}-values as the one determined before[9] from the $^{16}O + ^{63}Cu$ case (Fig. 1 and Table I) give good predictions for these nucleon evaporation channels (Figs. 2-5). Nevertheless, the 2 and 3 α-particles deexcitation channels are not sensitive to the ℓ_{cr} parameter (because, in fact, these many-particles channels have large emission probabilities for low ℓ-partial waves[22]).

Thus, the statistical evaporation code ALICE cannot reproduce correctly the experimental deexcitation channels for the $^{34}S + ^{45}Sc$ system, unless a supplementary assumption is introduced in the calculations, as for example, preequilibrium α-emissions[10]. However, the validity of this preequilibrium ALICE model dependent assumptions is seriously questionable. On one hand, because the experimental results[23, 24] concerning this preequilibrium process have been observed only for light ions (C, N, O and F) and at much higher incident energies ($E/A \sim 6$ MeV) than the ^{34}S-ones. On the other hand, because the desagreement between predictions and experimental results may be due to the shortcomings of the ALICE calculation.

As it was discussed before, if a compound nucleus is formed in the vicinity of the Yrast line, the γ-ray emission is predominant in this region[6] . Nevertheless, if the γ-ray deexcitation channel is not taken in account, nucleon emission will certainly take place in this region and, consequently, the corresponding emission probabilities will be overestimated with respect to the exact statistical calculations. Moreover, the α-particles emission will correspondingly be strongly hindered in this region and their cross sections will be underestimated. This seems to be the case for the $^{34}S + ^{45}Sc$ analysis using

the code ALICE.

Thus, more sophisticated statistical calculations including γ-ray emissions must be performed in order to test the above-discussed ALICE-model independent entrance channel critical angular momentum for the ^{79}Rb compound nucleus, as well as the preequilibrium assumptions in the $^{34}S + ^{45}Sc$ system.

II - THE CODE JULIAN

II-1. Method of calculations

Calculations were performed with the Monte-Carlo statistical code JULIAN[7,12], which follows the correct procedure for angular momentum coupling at each stage of deexcitation.

The compound nucleus can deexcite by particle (n, p, α) or/and γ-ray emissions. Fission competition was introduced by A. GAVRON[12], who has taken the same subroutine of the code ALICE. For any specific bombarding energy, the cross section for the compound nucleus formation may be calculated either by an optical model calculation or given as compound nucleus spin distribution $\sigma_\ell(E^*)$.

The transmission coefficients for light particles are calculated by the subroutine ABACUS II, using optical model potentials from Ref. 25 (the same as in the code ALICE), whose values are very close of the PEREY systematics[26]. Yet, two options can be chosen in the program : in the first one[7], the transmission coefficients are calculated at each step for every emitted particle. In the second one[12], they are obtained during the first step of deexcitation and extrapolations are made for the subsequent stages of deexcitation from the initial ones.

The calculations were performed for 500 deexcitation cascades (events). The particles emission probabilities are calculated by Eq.(5), the γ-ray emission by Eq. (6). The normalization constants ξ_L were determined from Ref. 28 and were chosen as 0,1 Weisskopf units for E_1 and M_2 and 50 for E_2 transitions.

The binding energies of the emitted particles are those of the Wapstra tables[27]. The level densities are calculated with the Lang formula[17] (Eqs. I-2).

For calculations performed with the Gavron approximation[12], the level density $\rho(E^*,J)$ used in these calculations above $E^* \sim 5$ MeV is given by :

$$\rho(E^*,J) = \rho_o(U)\ (2J+1)\ \exp\{2\ [a(U - E_{ROT}\ (J))]^{1/2}\} \qquad (7)$$

where $U = E^* - P$, P is the pairing energy and $\rho_o(U)$ is taken from Gilbert Cameron formalisme[29] :

$$\rho_o(U) = \frac{\sqrt{\pi}}{\sqrt{12}}\ \frac{\exp(2\sqrt{aU})}{a^{1/4}\ U^{5/4}}\ \frac{1}{\sqrt{2\pi}\ \sigma} \quad , \qquad (8)$$

σ being the spin cut-off :

$$\sigma^2 = \mathcal{I}_T/\hbar^2 \ . \qquad (9)$$

For the sake of simplicity, this latter calculations will be named JULIAN 2 and JULIAN 1 for the former one.

The level density parameter "a" was taken, whatever the option, from the Gilbert Cameron[29] expression :

$$a/A = 0{,}00917\ S + K\ (MeV^{-1}) \qquad (8)$$

In the above relation, $S = S_N + S_P$ is the shell correction for protons and neutrons, taken from Ref.29, K is a parameter representing the shape of the nuclei : the average value[29] K = 0,131 was chosen in the calculations (nuclei slightly deformed).

When calculations are performed with compound nucleus cross section being calculated by the code JULIAN, the cross sections for the deexcitation channels are systematically underestimated by the calculations for both $^{16}O + {}^{63}Cu$ and $^{34}S + {}^{45}Sc$ systems. This is due to the fact that the compound nucleus cross sections calculated by the optical model subroutine are smaller

than the experimental results for both $^{16}O + ^{63}Cu$ and $^{34}S + ^{45}Sc$ reactions (Fig.6). So, in order to avoid this underestimation of the compound nucleus cross sections, the compound nucleus spin distribution calculated by the code ALICE was given as input for JULIAN calculations. Indeed, although the exit channels is not correctly reproduced by the code ALICE, the experimental complete fusion cross section is in close agreement with the predictions of this code (Fig. 6).

II-2. Comparison with experimental results

A : $^{16}O + ^{63}Cu$

The comparison between predictions and experiments for the $^{16}O + ^{63}Cu$ system is shown in the Figs. 7-10 for both calculations performed[7,12]. As seen in these figures, a better overall agreement is found with the JULIAN 1 calculations. Indeed, although JULIAN 2 gives better agreement for the pn-channel, the predicted cross sections for all others channels are shifted to lower compound nucleus excitation energies with respect to the experimental ones. Yet, the maxima of the cross section for almost all channels are not reproduced by Gavron's calculations. The disagreement is partially due to the Gilbert-Cameron level density relation used in these calculations. Indeed, numerical calculations[31] have shown that predictions of the Gilbert-Cameron relation overestimate the level density for high angular momentum. But, rather than only blaming the Gilbert-Cameron level density predictions, the approximation in the transmission coefficients could also be questioned. On the other hand, the calculations performed with JULIAN 1 give a very good agreement with the $^{16}O + ^{63}Cu$ experimental results.

But the most important feature concerning the predictions of the code JULIAN is that no critical angular momentum assumption is need to obtain agreement with the experimental results for the ^{79}Rb compound nucleus deexcitation channels formed in the $^{16}O + ^{63}Cu$ reaction, at least for almost all exit channels (Figs. 7-10). Indeed, JULIAN 1 calculations overestimate the pxn-channels almost systematically, while the 3pn-one is correspondingly underestimated. However, before searching critical angular momentum effects in these channels, it must be reminded that the calculations are very sensitive to the γ-ray normalization constants ξ_L and the values taken in the calculations are those

extracted from low-lying single states at low excitation energies[28], so they are subject to large uncertainties when applied to high excitation energy and high spins. On the other hand, the predictions of the code JULIAN are subject to statistical uncertainties due to the Monte-Carlo statistical procedure[30] of this evaporation code. So, smaller a predicted cross section is, greater will be its statistical incertitude, and to overcome this restriction, a mean value has to be taken over a lot of identical calculations performed for each energy. However, it is noted that the treatment of ^{79}Rb at, for example, 68 MeV excitation energy with a spin distribution reaching 51 ħ in the entrance channel took 35 min with a UNIVAC 1110 computer.

Thus, the minor differences observed between JULIAN 1 predictions and experimental results for the $^{16}O + ^{63}Cu$ system are most probably caused by the above-discussed factors and very probably the introduction of a critical angular momentum should be unecessary. Hence, this result shows the importance of taking into account the γ-ray deexcitation channels in the statistical model calculations, besides more exact relations for the level densities and emission probabilities.

B : $^{34}S + ^{45}Sc$

The results concerning the $^{34}S + ^{45}Sc$ reaction are shown in Figs. 11-14 where predictions and experimental results are shown as a function of the ^{79}Rb compound nucleus excitation energy. For this system, only the exact calculations of the code JULIAN (JULIAN 1) was performed. Yet, the calculations were performed with the same set of parameter values as for the $^{16}O + ^{63}Cu$ system (see above), while the compound nucleus entrance channel spin distribution σ_ℓ, was taken from the code ALICE.

A very good agreement is found between predictions and experimental results for this system. As already observed, and discussed, the code overestimates slightly the pxn-channel in the same way as in $^{16}O + ^{63}Cu$ system, but no critical angular momentum parameter is needed to obtain agreement for the few-nucleon evaporation channels. Thus, as found in the above analysis of the $^{16}O + ^{63}Cu$ system, nearly all partial ℓ-waves in the entrance channel go on the compound nucleus cross section, a result that was already found in direct comparison of identical deexcitation channels for both systems[14].

However, the most important feature concerning the $^{34}S + ^{45}Sc$ system is that the calculations reproduce correctly the cross section for the many-particles evaporation channels (Fig. 14), a result which rejects definitively the precquilibrium assumption suggested above (section I.2). This result shows in fact that the code JULIAN calculates correctly the emission probabilities for all possible deexcitation channels. On the other hand, the importance of the γ-ray channels is observed again in these results, as the γ-ray competition in the compound nucleus decay is a stabilizing factor on the nucleon-α particle competition.

CONCLUSIONS

This work has shown that measurements of individual deexcitation channels in a compound nucleus decay is of great importance to check the validity of the several assumptions included in the statistical evaporation codes. From the comparison between the experimental excitation functions for the $^{16}O + ^{63}Cu$ and $^{34}S + ^{45}Sc$ compound nucleus reaction and the predictions of the codes ALICE and JULIAN for both systems, it is concluded that the code ALICE do not predict correct cross sections if no further assumptions are introduced in the calculations. Thus, a critical angular momentum energy dependent parameter has to be introduced in the ALICE calculations to obtain agreement with the $^{16}O + ^{63}Cu$ results. For the $^{34}S + ^{45}Sc$, besides this critical angular momentum assumption, a preequilibrium process has to be also introduced to obtain agreement between predictions of the code ALICE and many-particles evaporation channels.

On the other hand, the code JULIAN gives correct predictions for both systems if calculations are performed with the Lang level density relation and global light particles transmission coefficients calculations (JULIAN 1). These predictions are obtained without any assumptions, as that above discussed, and with a fixed set of parameters values for both $^{16}O + ^{63}Cu$ and $^{34}S + ^{45}Sc$ systems.

From these results, it is concluded that the γ-ray deexcitation channels must be taken into account if experimental results are to be correctly compared to statistical calculations. Thus, calculations performed with the code ALICE must be used with great care, since the γ-ray channel is neglected.

It is also clearly important to extend this type of comparison to other statistical evaporation codes, as GROGI[6] and CASCADE[8], in order to conclude as to which calculation is closest to the experimental results. This work is under way[22].

The authors are indebted to Dr. D. GUERREAU for helpful comments and to Dr. F. PLAGNOL for a critical reading of the text.

REFERENCES

1. V.F. Weisskopf and D.H. Ewing, Phys. Rev. 57, 472 (1940).
2. W. Hauser and H. Feshbach, Phys. Rev. 87, 366 (1952);
A.M. Lane and R.G. Thomas, Rev. Mod. Phys. 30, 257 (1958).
3. T. Ericson, Advan. Phys. 9, 425 (1960) ;
D.W. Lang and K.J. Le Couteur, Nucl. Phys. 14, 21 (1960).
4. Cohen, Plasil and Swiatecki, Ann. Phys. (N.Y.) 82, 557 (1974).
5. M. Blann and F. Plasil,
ALICE : A Nuclear Evaporation code. USAEC Report COO 3494-10 (1973) ;
Phys. Rev. Lett. 29, 303 (1972).
6. J.R. Grover and J. Gilat, Phys. Rev. 157, 802, 814, 823 (1967).
7. M. Hillmann and Y. Eyal, in proceedings of the European Conference on Nuclear Reactions with heavy Ions, Caen (France), 1976, 109.
8. F. Pühlhofer, Nucl. Phys. A 280, 267 (1977).
9. M. Langevin, J. Barreto and C. Détraz, Phys. Rev. C14, 152 (1976).
10. M. Langevin, J. Barreto, C. Détraz and J. Vernotte, in proceedings of the European Conference on Nuclear Reactions with heavy Ions, Caen (France), 1976, 108.
11. S. Della Negra, H. Gauvin, H. Jumeglas, Y. Le Beyec and M. Lefort, Z. Physik A282, 282 (1977).
12. A. Gavron, Phys. Rev. C21, 230 (1980).
13. J. Galin, B. Gatty, D. Guerreau, U.C. Schlotthauer-Vos and X. Tarrago, Phys. Rev. C10, 638 (1974).
14. J. Barreto, M. Langevin and C. Détraz, Report IPNO-PhN 80-07.
15. M. Blann, Corrections to overlaid ALICE, UR-NSRL 181 ; Report COO-3494-29.
16. D.T. Thomas, Phys. Rev. 116, 703 (1959).
17. D.W. Lang, Nucl. Phys. 26, 434 (1961).

18. D.T. Thomas, Nucl. Phys. 53, 558, 577 (1964) ;
Annu. Rev. Nucl. Sci. 18, 343 (1968).

19. D.C. Williams and T.D. Thomas, Nucl. Phys. A92, 1 (1967).

20. D. Guerreau, Thèse Doctorat es-sciences, Université Paris-Sud (1973), and private communication.

21. M. Delagrange, F. Hubert and A. Fleury, Nucl. Phys. A228, 397 (1974).

22. J. Barreto, Thèse Docteur d'Etat, Université Parix XI (unpublished).

23. D.G. Sarantites, L. Westeberg, M.L. Halbert, R.A. Dayras, D.C. Hansley and J.H. Barker, Phys. Rev. C18, 774 (1978) ;
L. Westeberg, D.G. Sarantites, D.C. Hansley, R.A. Dayras, M.L. Halbert and J. Barker, Phys. Rev. C18, 796 (1978).

24. T. Inamura, M. Ishihara, T. Fakuda and T. Shimoda. Phys. Lett. 69B, 51 (1977) ;
D.R. Zolnowski, Y. Yamada, S.E. Cala, A.C. Kalher and T. Sugihara, Phys. Rev. Lett. 41, 92 (1978).

25. G.S. Mani, M.A. Melkanoff and I. Iori, Proton and neutron penetrabilities using an optical model potential, report CEA N° 2379 and 2380 (1963).

26. C.M. Perey and F.G. Perey, at Nucl. Data Tables 17, 1 (1976).

27. A.H. Wapstra and N.B. Gove, Nuclear Data Tables 19, 4-5 (1971) ;
A.H. Wapstra and K. Bos, Atomic Data and nuclear data tables 19, 3 (1977).

28. F. Bertrand, M. Martinot and N. Vergès, Nuclear Data in Science and Technology, 2, 353 (1973).

29. A. Gilbert and A.G.W. Cameron, CAN. J. of Phys. 43, 1446 (1965).

30. Antonio D'Onofrio, Thèse Docteur 3ème Cycle, Université Paris XI (unpublished).

31. M. Hillmann and J.R. Grover, Phys. Rev. 185, 1303 (1969).

TABLE I

CRITICAL ANGULAR MOMENTUM ℓ_{cr}-VALUES FOR THE $^{16}O + {}^{63}Cu$ and $^{34}S + {}^{45}Sc$ COMPOUND NUCLEUS REACTIONS

	E^* (MeV)	$\ell_{max}(\hbar)$	ALICE $\ell_{cr}(\hbar)$ [a]	EXP $\ell_{cr}(\hbar)$ [b]
$^{16}O + {}^{63}Cu$	32.0	9	9	-
	36.0	18	18	-
	40.0	23	22	-
	43.8	28	24 ± 1	23 ± 1.5
	47.8	32	26 ± 1	27 ± 2.0
	52.0	35	28 ± 1	31 ± 3.0
	56.0	37	30 ± 1	33 ± 2.5
	60.0	40	32 ± 1	35 ± 2.5
	63.7	42	34 ± 1	39 ± 3.0
	67.4	43	36 ± 1	40 ± 3.0
$^{34}S + {}^{45}Sc$	48.3	19	19	13 ± 2.0 [b]
	51.1	28	28	21 ± 2.5
	56.8	37	31 ± 1	32 ± 3.0
	62.5	43	33 ± 1	39 ± 4.0
	68.2	49	35 ± 1	43 ± 4.0
	73.9	54	37 ± 1	53 ± 5.0

a) reference 9

b) reference 14

FIGURE CAPTIONS

1. Comparison between various experimental results for the $^{16}O + ^{63}Cu$ (ref. 9) and predictions of the code ALICE. The solid line curves are drawn through the experimental points. The predictions of the code ALICE are represented by a dashed-dot line when calculations are performed under the assumption $\sigma_{CN} = \sigma_R$ and by a dashed line when contributing partial waves are restricted to $\ell \leq \ell_{cr}$ (see text).

2. Comparison between experimental pxn and 2p evaporation channels for the $^{34}S + ^{45}Sc$ system and predictions of the code ALICE (see Fig. 1 caption). The effect of changing ℓ_{cr} by 1 $\hbar$ is indicated for the pn-channel. Predictions of the ALICE calculations performed with $a = A/6$ is shown for the 2p-channel.

3. Comparison between experimental 2pxn + αxn evaporation channels for the $^{34}S + ^{45}Sc$ system and predictions of the code ALICE (See caption Fig.1).

4. Comparison between experimental αpxn and α2pn evaporation channels for the $^{34}S + ^{45}Sc$ system and predictions of the code ALICE (See caption Fig. 1).

5. Comparison between experimental 2αxn, 2αpn and 3αn evaporation channels for the $^{34}S + ^{45}Sc$ systems and predictions of the Code ALICE (See caption Fig. 1). Predictions of the ALICE calculations performed with $a = A/6$ is shown for the 2αn channel.

6. Absolute experimental compound nucleus cross section for the $^{16}O + ^{63}Cu$ and $^{34}S + ^{45}Sc$. The solid line curves represents the predictions of the Code JULIAN with optical model parameters from ref.26 (see text) ; the dashed line curves are the predictions of the code ALICE.

7. Comparison between experimental 2n and pxn evaporation channels for the $^{16}O + ^{63}Cu$ system and predictions of the Code JULIAN. The solid line curves are the predictions of calculations with Lang level density formula and complete transmission coefficients calculations for the

emitted particle (JULIAN 1) ; the dotted line curves are predictions of the Gilbert-Cameron level density formula and partial transmission coefficients calculations (JULIAN 2).

8. Comparison between 2pxn and 3pn evaporation channels for the $^{16}O + ^{63}Cu$ system and predictions of the code JULIAN (See caption Fig. 7).

9. Comparison between αxn and αpxn evaporation channels for the $^{16}O + ^{63}Cu$ system and predictions of the Code JULIAN (See caption Fig. 7).

10. Comparison between α2pn, 2αxn and 2αpn evaporation channels for the $^{16}O + ^{63}Cu$ system and predictions of the Code JULIAN (See caption Fig.7).

11. Comparison between pxn and 2p evaporation channels for the $^{34}S + ^{45}Sc$ system and predictions of the code JULIAN (See text).

12. Comparison between 2pxn and αxn evaporation channels for the $^{34}S + ^{45}Sc$ system and predictions of the code JULIAN (See text).

13. Comparison between αpxn and α2pn evaporation channels for the $^{34}S + ^{45}Sc$ system and predictions of the code JULIAN (See text).

14. Comparison between 2αxn, 2αpn and 3αn evaporation channels for the $^{34}S + ^{45}Sc$ system and predictions of the code JULIAN (See text).

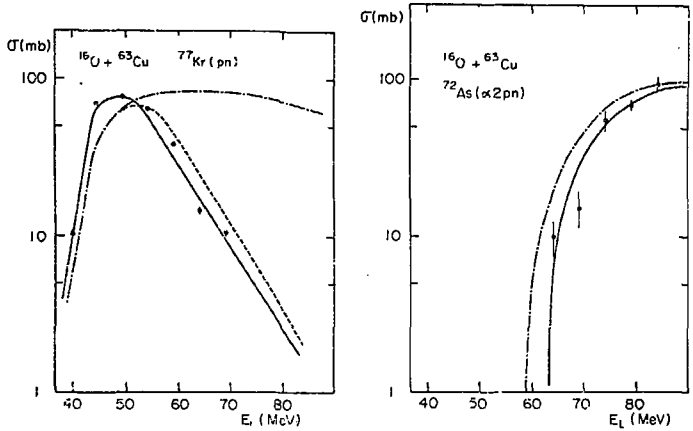
σ(mb)
$^{16}O + ^{63}Cu$ ^{77}Kr (pn)
100
10
1
40
50
60
70
80
E_L (MeV)
σ(mb)
$^{16}O + ^{63}Cu$
^{72}As (α2pn)
100
10
1
40
50
60
70
80
E_L (MeV)

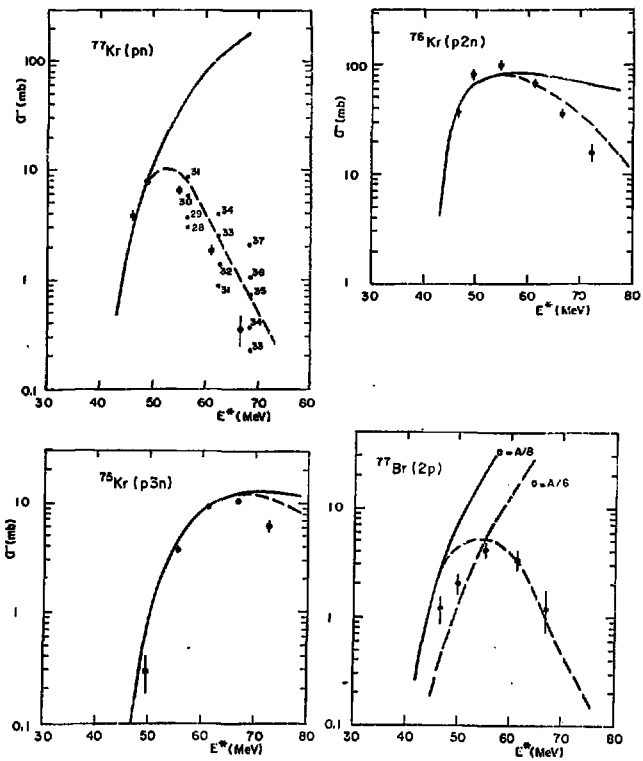
77Kr (pn)
76Kr (p2n)
75Kr (p3n)
77Br (2p)
σ (mb)
E* (MeV)
a = A/8
a = A/6

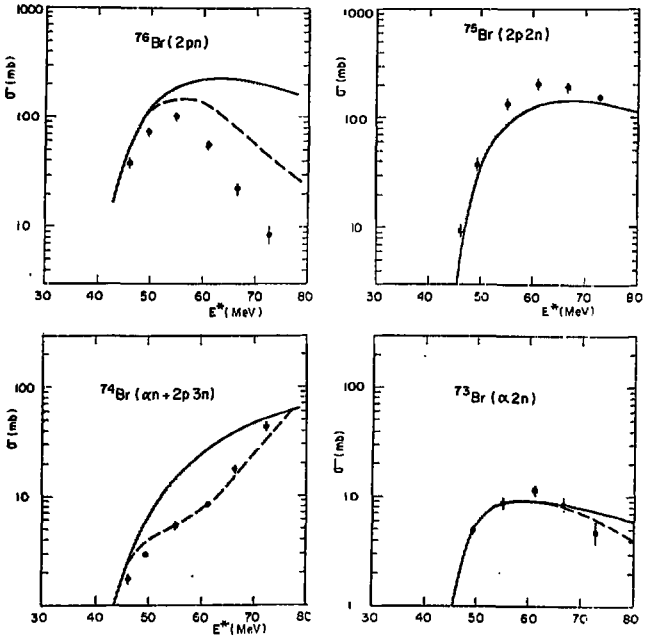
^{76}Br (2pn)
^{75}Br (2p2n)
^{74}Br (αn + 2p3n)
^{73}Br (α2n)
σ (mb)
E* (MeV)

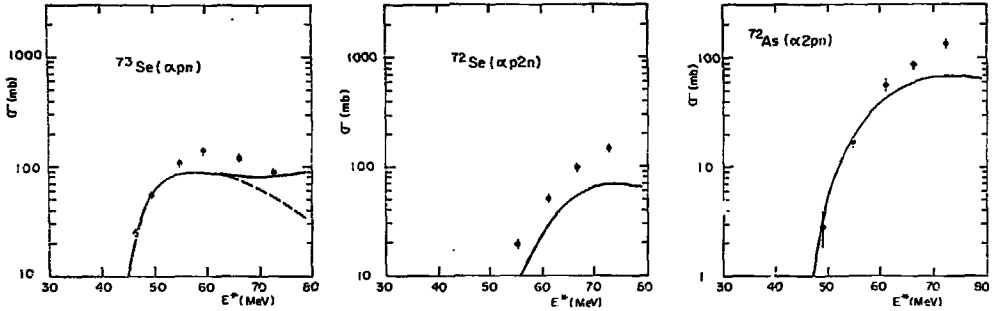
^{73}Se(α,pn)
^{72}Se(α,p2n)
^{72}As(α,2pn)
σ (mb)
E* (MeV)
1000
100
10
1
30
40
50
60
70
80
90

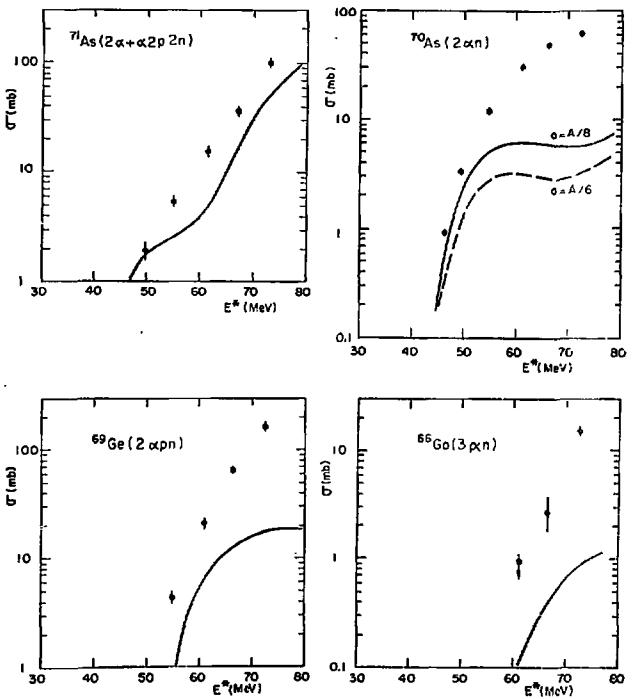
^{71}As(2α+α2p 2n)
^{70}As(2αn)
^{69}Ge(2αpn)
^{65}Go(3pαn)
σ (mb)
E* (MeV)
σ=A/8
σ=A/6

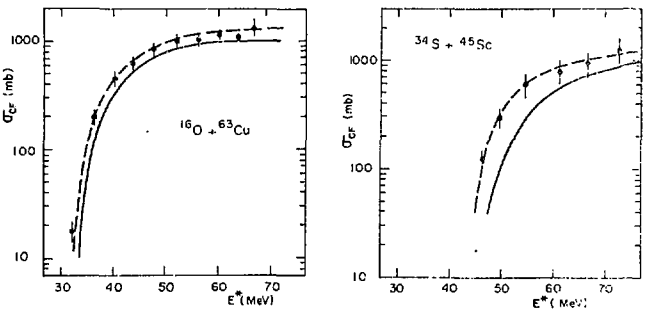
1000
100
10
σ_{CF} (mb)
$^{16}O + ^{63}Cu$
30
40
50
60
70
E*(MeV)
$^{34}S + ^{45}Sc$
1000
100
10
σ_{CF} (mb)
30
40
50
60
70
E*(MeV)

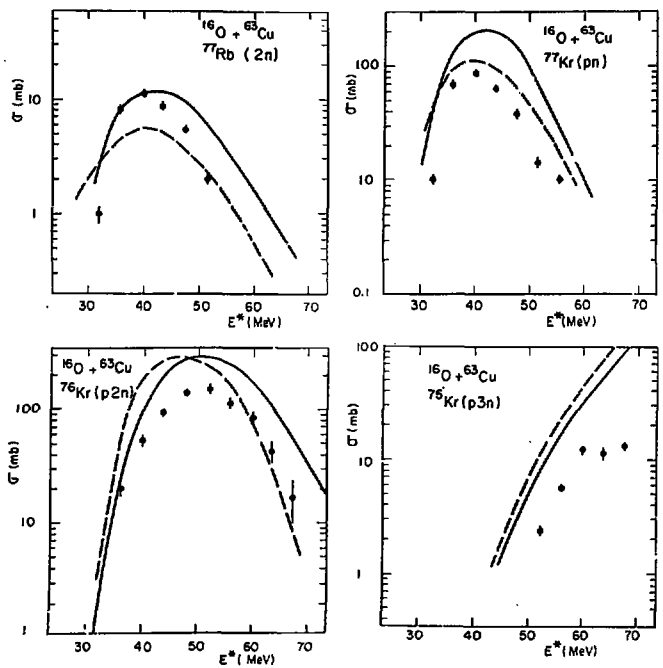
$^{16}O + ^{63}Cu$
^{77}Rb (2n)
$^{16}O + ^{63}Cu$
^{77}Kr (pn)
$^{16}O + ^{63}Cu$
^{76}Kr (p2n)
$^{16}O + ^{63}Cu$
^{75}Kr (p3n)
σ (mb)
σ (nb)
E* (MeV)

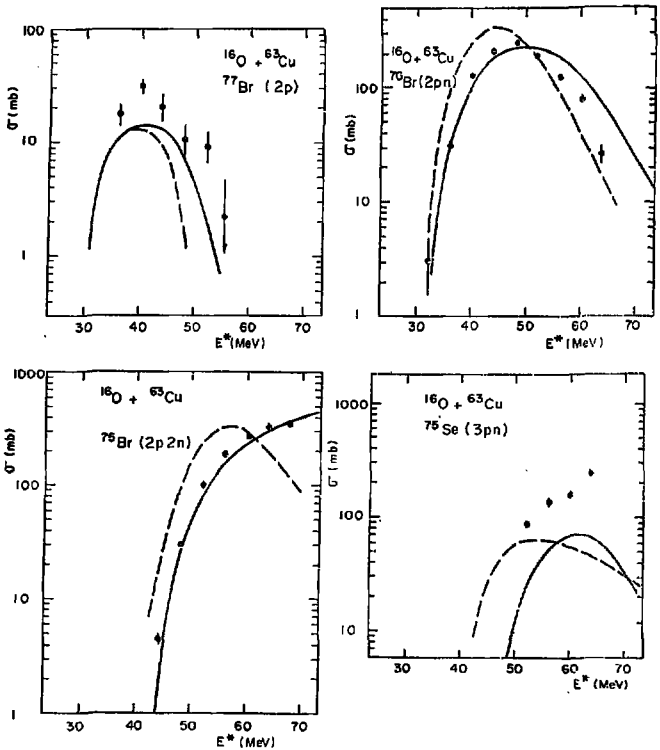
$^{16}O + ^{63}Cu$
^{77}Br (2p)
$^{16}O + ^{63}Cu$
^{70}Br(2pn)
$^{16}O + ^{63}Cu$
^{75}Br (2p2n)
$^{16}O + ^{63}Cu$
^{75}Se (3pn)
σ (mb)
E* (MeV)

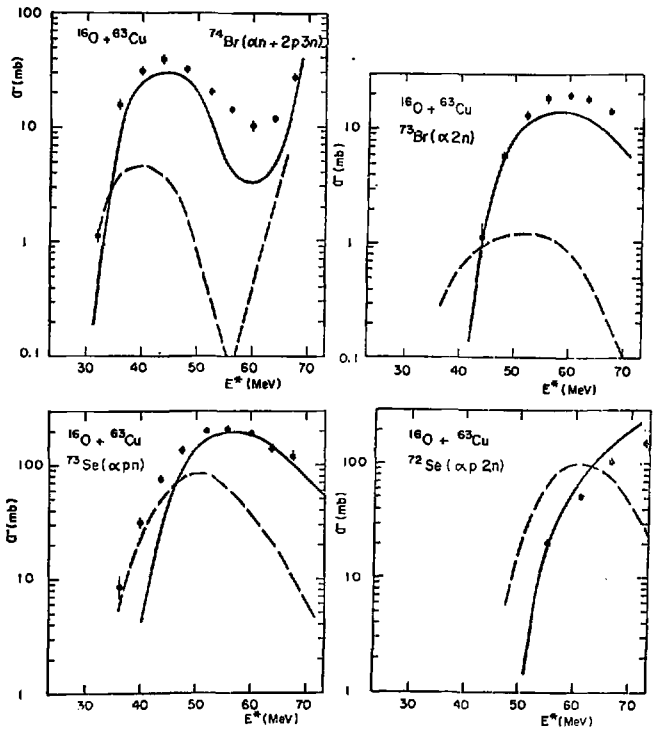
$^{16}O + ^{63}Cu$
$^{74}Br(\alpha n + 2p3n)$
$^{16}O + ^{63}Cu$
$^{73}Br(\alpha 2n)$
$^{16}O + ^{63}Cu$
$^{73}Se(\alpha pn)$
$^{16}O + ^{63}Cu$
$^{72}Se(\alpha p 2n)$
σ (mb)
E* (MeV)

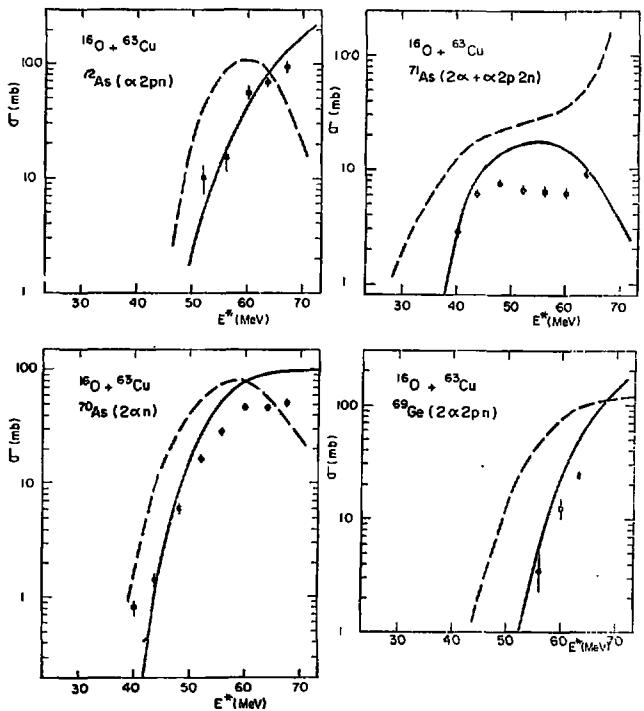
$^{16}O + ^{63}Cu$
^{72}As ($\alpha 2pn$)
$^{16}O + ^{63}Cu$
^{71}As ($2\alpha + \alpha 2p\,2n$)
$^{16}O + ^{63}Cu$
^{70}As ($2\alpha n$)
$^{16}O + ^{63}Cu$
^{69}Ge ($2\alpha 2pn$)
σ (mb)
E^*(MeV)

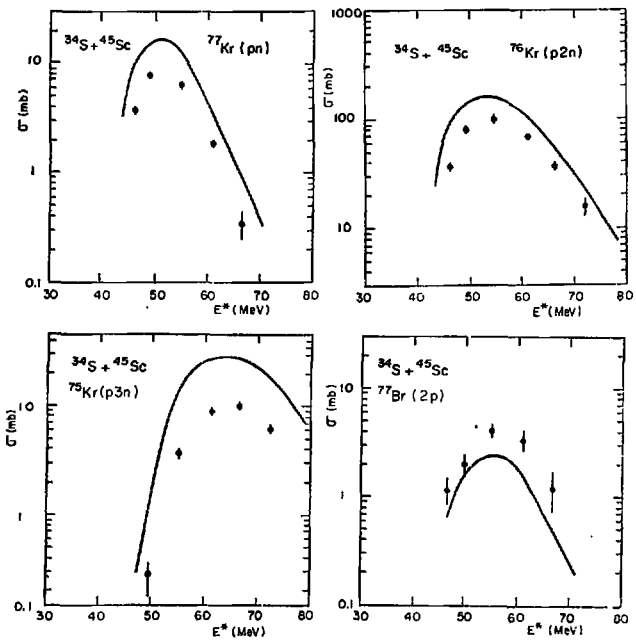
$^{34}S + ^{45}Sc$
^{77}Kr (pn)
$^{34}S + ^{45}Sc$
^{76}Kr (p2n)
$^{34}S + ^{45}Sc$
^{75}Kr(p3n)
$^{34}S + ^{45}Sc$
^{77}Br (2p)
σ (mb)
E* (MeV)

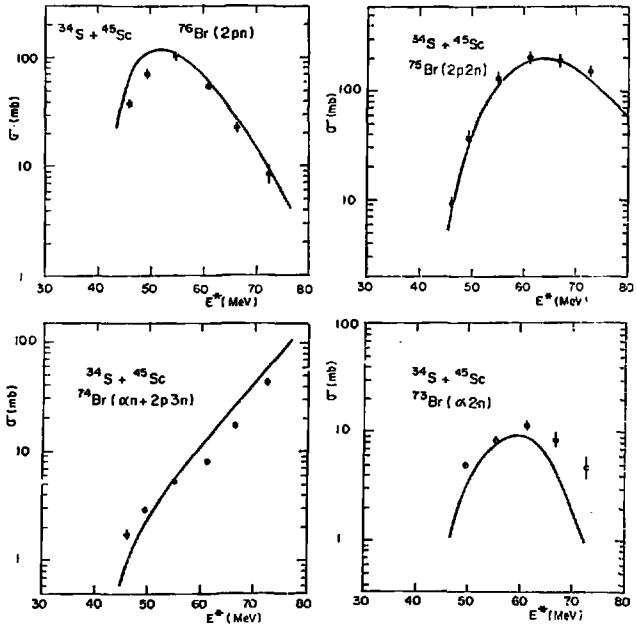
$^{34}S + ^{45}Sc$
^{76}Br (2pn)
$^{34}S + ^{45}Sc$
^{75}Br (2p2n)
$^{34}S + ^{45}Sc$
^{74}Br (αn + 2p3n)
$^{34}S + ^{45}Sc$
^{73}Br (α2n)
σ (mb)
E* (MeV)

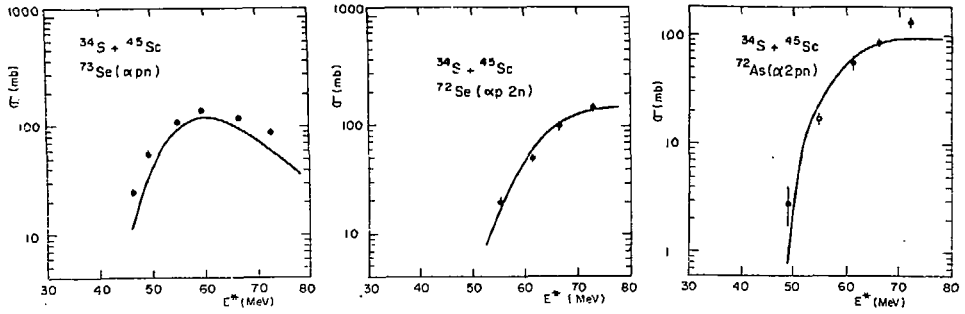
$^{34}S + ^{45}Sc$
$^{73}Se(\alpha pn)$
$^{34}S + ^{45}Sc$
$^{72}Se(\alpha p\,2n)$
$^{34}S + ^{45}Sc$
$^{72}As(\alpha 2pn)$
σ (mb)
E* (MeV)

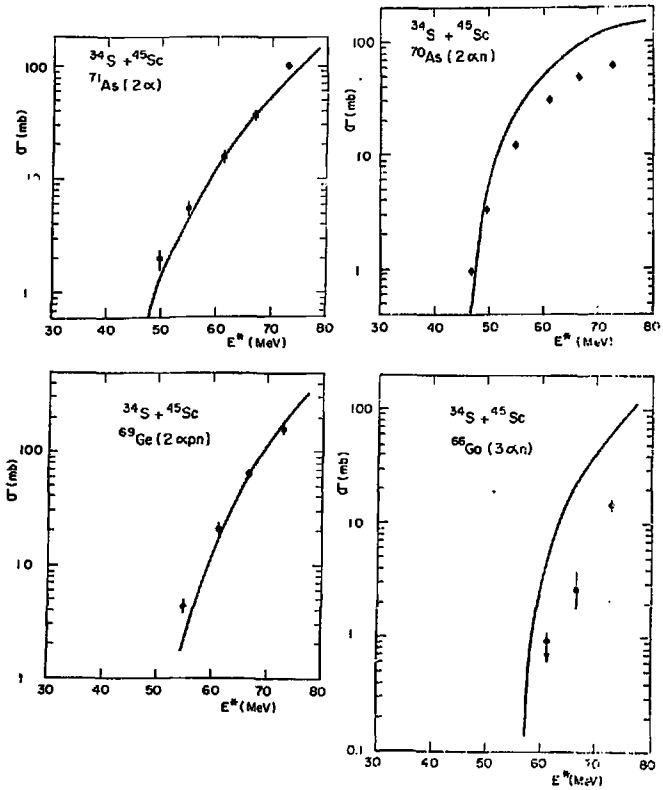
$^{34}S + ^{45}Sc$
^{71}As (2α)
$^{34}S + ^{45}Sc$
^{70}As (2αn)
$^{34}S + ^{45}Sc$
^{69}Ge (2αpn)
$^{34}S + ^{45}Sc$
^{66}Ga (3αn)
σ (mb)
E^* (MeV)